Picturing Schmitt's trigger

Bryan Hart takes an in-depth look at a sixty-year-old device that most designers today take for granted – the Schmitt trigger.

In digital system design the normally preferred shape of a waveform resembles that of **Fig. 1a)**. The waveform is 'clean' When the digital signal v_S represents a '0', in the positive logic convention, it has a constant level V_{OL} in the acceptable '0' range. Similarly, a '1' is represented by a constant level V_{OH} in the acceptable '1' band.

Furthermore, transitions between levels are 'smooth' Mathematically, the signal is said to increase monotonically from '0' to '1' and decrease monotonically from '1' to '0'

However, as a result of crosstalk in interconnecting wires a practical waveform could resemble that shown in Fig. **1b)**. Noise 'spikes' p, q, are shown as occurring after the main transitions but they could appear during the transitions themselves as a result not only of crosstalk but also of ringing on interconnection paths.

Spikes p and q might jeopardise intended system operation, so how can they be eliminated? The use of a differential voltage comparator might seem to be appropriate, so consider **Fig. 2**, in which Fig 1b) is repeated for convenience. The noise-contaminated waveform is applied to the non-inverting input of the comparator, C_O, in Fig. **2b)**: C_O is assumed to have ideal static and dynamic characteristics.

If the comparator reference level V_R, applied to the inverting input, is set at V_X then the output is as shown in Fig. **2c)**

Spike q is ignored but p causes two output pulses to appear instead of the single one required.

Similar conditions hold when $V_R = V_Y$, but in that case p is ignored not q. For the waveform illustrated , with $v_P < v_Q$, it is not possible to eliminate the effects of both p and q using a comparator as a straightforward clipper/limiter.

The problem can be solved using a scheme known as a Schmitt trigger[1]. Long before the advent of modern digital electronics, this name was given to a particular comparator circuit based on a pair of cathode-coupled thermionic tubes

Originally, the Schmitt trigger was designed to produce abrupt changes in output voltage for slowly varying input signals. Nowadays the name is used to describe a generic circuit function, rather than a particular component assembly, though some form of comparator with a long-tailed pair input stage is commonly employed in bipolar transistor designs.

The purpose of this article is twofold: to explain some features of Schmitt-trigger operation which, though important in innovative design, are ignored in the general literature; to show how the Schmitt trigger can be designed to eliminate the effects of spikes p and q in Fig 1b.

How the trigger works

Whatever the details of the internal circuitry, the Schmitt trigger may be regarded, from a system viewpoint, as a differential voltage comparator with positive feedback. **Figure 3** shows this for the case of inverting-mode operation; the non-inverting case is mentioned, briefly, later.

Potential differences V_S, $\in$, V_O are the d.c. values of the signal voltage, differential input voltage and output voltage respectively.

A three section piecewise-linear approximation to the static transfer characteristic, of C_O itself, is shown in **Fig. 4** and a d.c. equivalent circuit for each region of operation is shown in the box above it.

In Regions 1, 3 corresponding to saturation, the output can be modelled by the batteries V_{HL}, V_{LL}, respectively. In Region 2, the linear or active region, the output is modelled by a voltage-controlled voltage generator For simplicity the

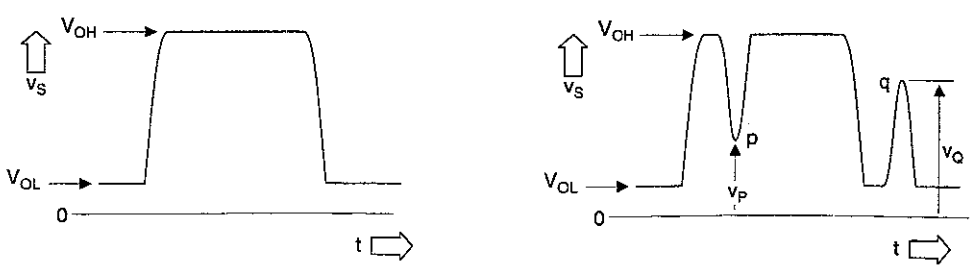

Fig. 1. Preferred shape of a binary signal, a), and possible shape, b), with noise spikes p, q.

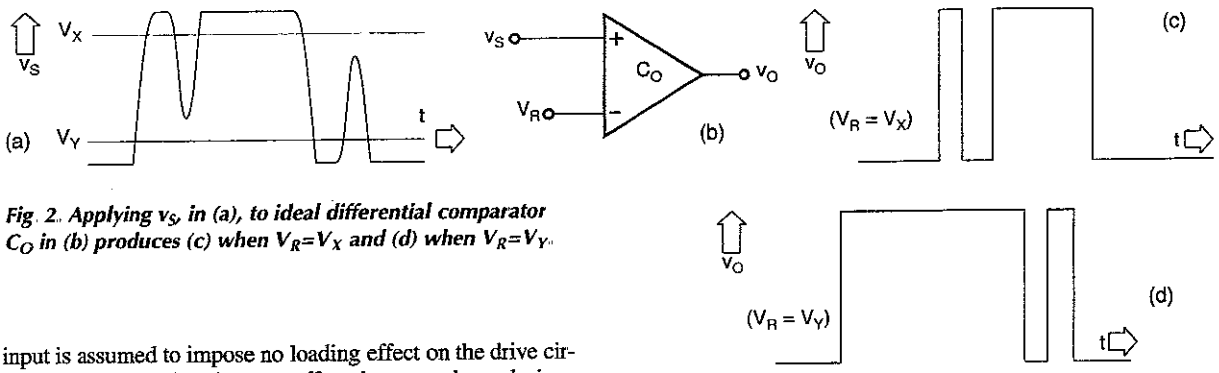

Fig. 2. Applying v_S, in (a), to ideal differential comparator C_O in (b) produces (c) when $V_R=V_X$ and (d) when $V_R=V_Y$.

input is assumed to impose no loading effect on the drive circuit. This assumption does not affect the general conclusions that are reached regarding system operation.

With the help of Fig 3, it can be determined that,

$$V_s = \in + \beta V_o \tag{1}$$

where,

$$\beta = \frac{R_1}{R_1 + R_2} \tag{2}$$

Rearranging eqn 1,

$$V_o = -\frac{\in}{\beta} + \frac{V_s}{\beta} \tag{3}$$

When plotted on the transfer characteristic, eqn 3 represents a straight line, with a slope $-1/\beta$, that passes through the axis point $\in = V_S$. I will call this the operating line.

See what happens for various values of V_S. Line 'a', in **Fig. 5**, shows conditions for an arbitrarily large negative value, V_{S1}, of V_S. The line cuts the transfer characteristic at a single point P_1, where $V_O=V_{HL}$. Following a small momentary change in $\in$, owing to circuit noise, the operating point returns to P_1 so this is a stable position of equilibrium.

Line 'b', for V_{S2} ($>V_{S1}$), cuts the transfer characteristic at three points. The stable operating point is P_2, where V_O is still equal to V_{HL}. The other two intersections do not yet represent possible operating points because the comparator can exist in only one of its three regions at a given time. Until V_S is sufficiently positive for C_O to operate in Region 2, that is presently in Region 1.

For $V_S=V_{S3}$ ($>V_{S2}$) the operating line meets the transfer characteristic at two points P_3, P'_3. At P_3, line 'c' is tangential to the transfer characteristic at one edge of Region 2 and C_O behaves as a linear amplifier with positive feedback.

A momentary positive change in $\in$, once again due to circuit noise, now causes a regenerative switching action to occur as Region 2 is traversed. This action ceases when V_O reaches a limit and the circuit settles down into a stable state, at P'_3 in Region 3. What happens in the switching process will be discussed later.

The words used to describe V_{S3} are 'upper trip' (or, trigger)

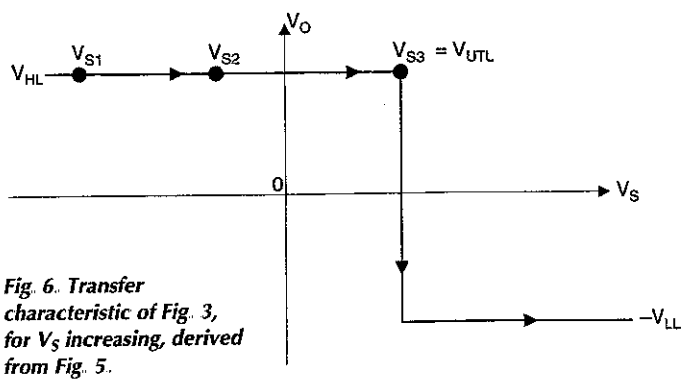

Fig. 6. Transfer characteristic of Fig. 3, for V_S increasing, derived from Fig. 5.

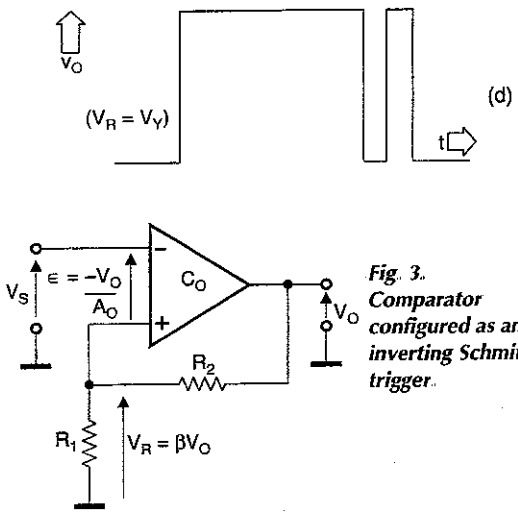

Fig. 3. Comparator configured as an inverting Schmitt trigger.

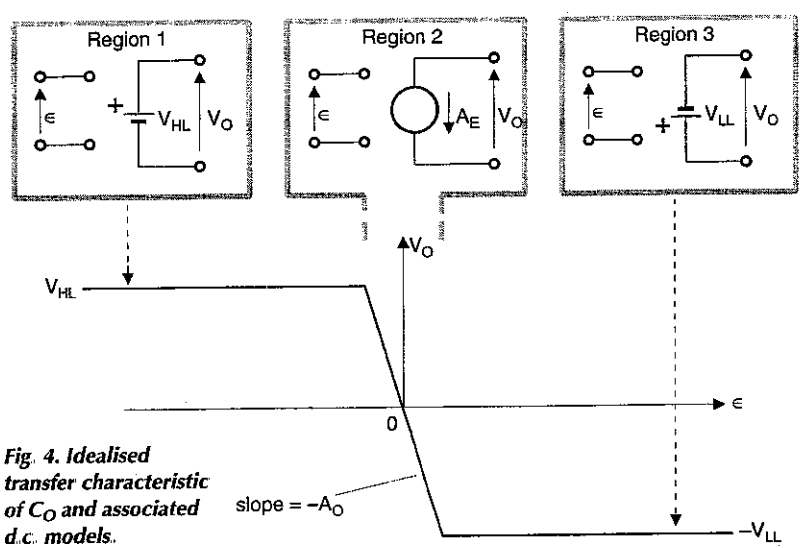

Fig. 4. Idealised transfer characteristic of C_O and associated d.c. models.

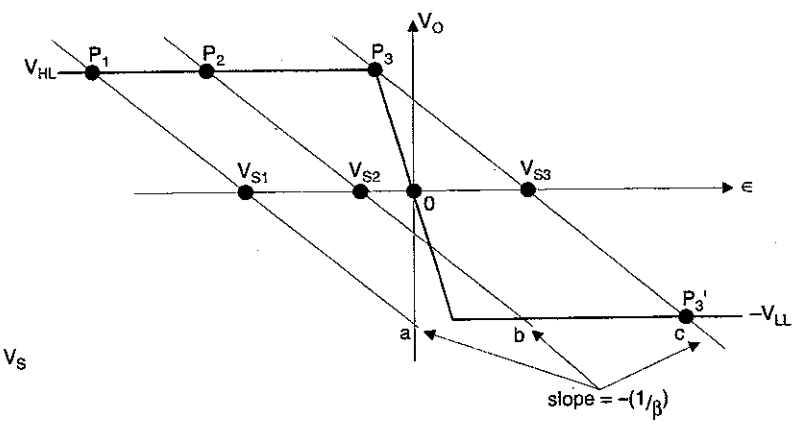

Fig. 5. Lines 'a', 'b', 'c' refer, respectively, to operation with $V_S=V_{S1}$, V_{S2} ($>V_{S1}$), V_{S3}($>V_{S2}$): $\beta=R_1/(R_1+R_2)$.

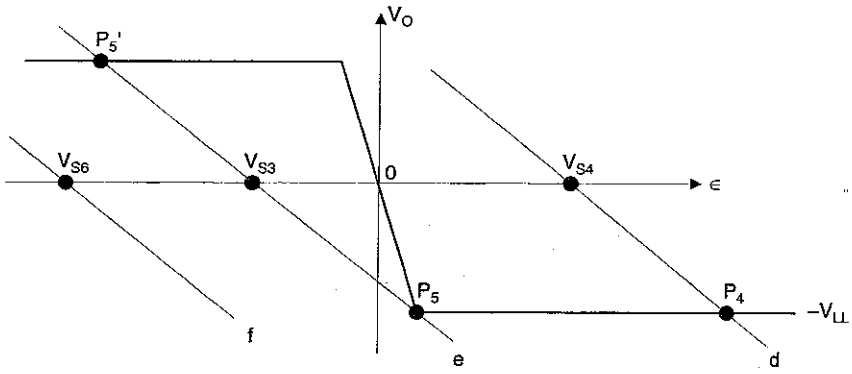

Fig. 7. Lines 'd', 'e', 'f', refer respectively to operation with $V_S=V_{S4}$, $V_{S5}(<V_{S4})$, $V_{S6}(<V_{S5})$.

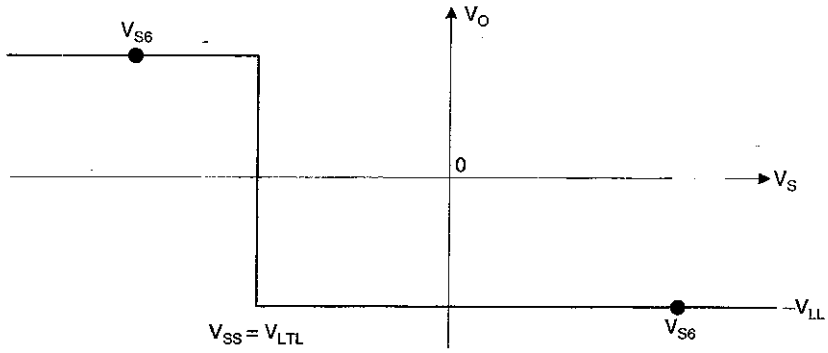

Fig. 8. Transfer characteristic of Fig. 3 for V_S decreasing, derived from Fig. 7.

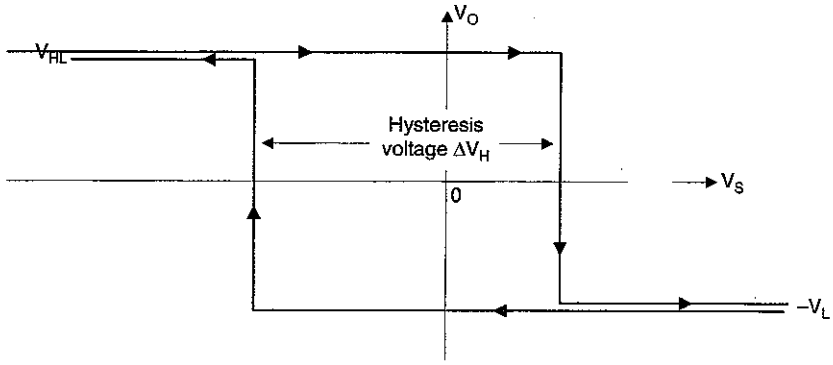

Fig. 9. The hysteresis characteristic is a composite plot of Figs 6, 8: the horizontal sections for $V_S<V_{LTL}$ and $V_S>V_{UTL}$ are shown slightly separated for clarity.

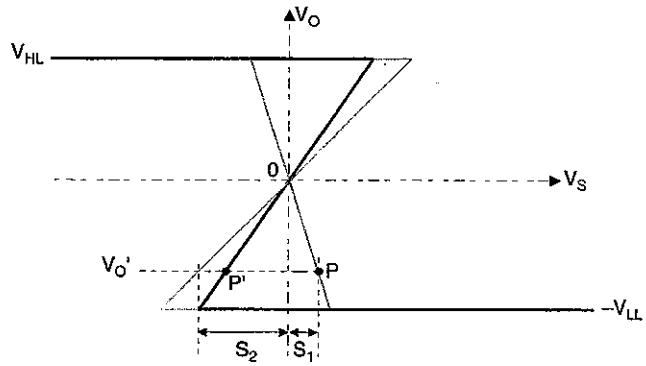

Fig. 10. Static transfer characteristic for Fig. 3 is shown bold. Line sections S_1, S_2 refer to terms in eqn 8.

level', and the letter subscripts UTL are used: thus, $V_{S3}=V_{UTL}$.

Substituting,

$$\epsilon = -\frac{V_{HL}}{\beta}$$

in eqn 3 and rearranging gives,

$$V_{S3} = V_{UTL} = -\frac{V_{HL}}{A_O} + (\beta V_{HL}) \tag{4}$$

For the normal case $\beta >> (1/A_O)$,

$$V_{UTL} \approx \beta V_{HL} \tag{5}$$

Derived from Fig. 5, **Figure 6** shows an apparent static plot of V_O *versus* V_S. The arrow direction indicates increasing V_S, and, if the input voltage is changing, increasing time, t.

In **Fig. 7**, which should be compared with Fig. 5, lines 'd', 'e' and 'f' show what happens when V_S decreases from a value V_{S4} ($>V_{S3}$). The output remains at $-V_{LL}$ till $V_S=V_{S5}$; then, 'e' is tangential to the transfer characteristic at point P_5 on the other edge of Region 2.

A tiny change in ϵ 1 due to circuit noise, is sufficient to initiate a regenerative switching action which ends when the point P'_5 in Region 1 is reached. **Figure 8** is derived from Fig. 7 in the same way that Fig. 6 is derived from Fig. 5. The arrow direction indicates successively decreasing values of V_S. If the input voltage is continually changing, this also corresponds to increasing t.

Voltage V_{S5} is designated 'lower trip (or trigger) level' and from reasoning similar to that which produced eqn 5,

$$V_{S5} = V_{LTL} \approx -\beta V_{LL} \tag{6}$$

Figure 9, a composite plot of Fig. 6 and Fig. 8, is the apparent static transfer characteristic of the system. The horizontal line sections for $V_S<V_{LTL}$ and $V_S>V_{UTL}$ should be shown coincident, but one is slightly displaced with respect to the other on this particular diagram to clarify the confusion that can arise when oppositely directed arrows are shown adjacent on the same line section

The system exhibits 'memory', characterised by a hysteresis, or deadband, voltage ΔV_H,

$$\Delta V_H = (V_{UTL} - V_{LTL}) \approx \beta(V_{HL} + V_{LL}) \tag{7}$$

Instead of the graphical procedure that led to Fig 9, you can obtain a plot of V_O versus V_S as follows.

At any point $V_S=V'_S$, $V_O=V'_O$ in Region 2, where,

$$\epsilon = -\frac{V'_O}{A_O}$$

Equation 1 can be rewritten as,

$$V'_S = -\frac{V'_O}{A_O} + (\beta V'_O) \tag{8}$$

Figure 10 shows a plot of the transfer characteristic, on which is constructed a line, with slope $1/\beta$, which passes through the origin. This line characterises the effect of feedback. At $V_O=V'_O$, V'_S is obtained by the algebraic addition of the horizontal line sections S_1 and S_2 that represent the two terms on the right-hand side of Fig. 8. Thus, point P' on the overall system characteristic corresponds to P on the transfer characteristic and the locus of points such as P' is the Z-shaped characteristic shown bold

The central section is a straight line of slope A'.

$$A' = \frac{-A_O}{1 - A_O\beta} \tag{9}$$

This equation follows from a rearrangement of eqn 8, or from the standard relationship for an amplifier with feedback[2]: for $\beta >> (1/A_O)$, $A' \approx 1/\beta$. It now seems that two different graphs describe the voltage transfer relationship for the

Schmitt trigger. Which one is correct?

Figure 10 relates to a d c model, only, of the system, i.e., the existence of energy storage elements is ignored. Hence, the effect of the regenerative action at $V_S=V_{UTI}$ and $V_S=V_{LTI}$ is not evident.

Figure 9, with the horizontal sections lying outside the hysteresis loop shown coincident, indicates the actual form of the trace observed in a practical sweep test designed to show V_O(Y) *versus* V_S(X), using a pen recorder or oscilloscope.

Incidentally, following on from Fig. 10, a three-dimensional plot of V_O (Y-axis) *versus* V_S (X) and β (Z) produces a folded surface similar to that encountered in elementary Chaos theory.

Some analogues in other areas of engineering science offer useful insight into the phenomenon of hysteresis. These are touched on next.

Analogues of hysteresis

The *BH* curve of a ferromagnetic material provides a familiar example of hysteresis. In that case it can be attributed to the 'remembered' angular orientation of domain magnetic moments.

An equivalent of hysteresis is the 'backlash' encountered in mechanical transmission systems, particularly those involving worn gear wheels, when the input drive is reversed. However, a more illuminating mechanical analogue is a see-saw with a sliding load.

Consider **Fig. 11**: this is a plan view of a light, rigid, beam pivoted in the middle. A smooth metal rod is attached to the side of the beam, like a curtain rail fixed to the wall above a window. A circular metal weight, *m*, similar to those used by weight-lifters, can slide freely along the rod between the end-stops situated at a distance L_1 to the left of the pivot and L_2 to the right.

Figure 12 is a side view of this see-saw scheme. A person, *n*-times heavier than weight *m*, walks from one end, G, towards the pivot, J, which is a height *h* above ground level. At this time the other end, K, is 2*h* above ground level.

When the person reaches a point L_1/n to the right of J, the beam starts to tip down on that side. This follows from the Principle of Moments. As it does so, *m* slides towards J, further aiding the motion of K towards the ground.

As the person walks back, **Fig. 13**, K does not move upward until he reaches a point L_2/n to the left of J. A 'transfer characteristic' for the mechanical operation is shown in **Fig. 14**: in this particular drawing, $n=2$.

Switching and stability

Referring back to Figs 5, 7 it is necessary to use a dynamic model of C_O to understand Schmitt-trigger behaviour on reaching points P_3, P_5. The simplest model, but one which highlights the main features of operation, is that shown within the broken-line triangular outline in **Fig. 15**.

The use of lower case letters indicates that voltage *changes* are being considered. Components *R* and *C* define a single-pole frequency response in Region 2. Thus,

$$A' = \frac{-A_O}{1 + j\dfrac{\omega}{\omega_c}} \qquad (10)$$

or,

$$A' = \frac{-A_O}{1 + j\omega\tau_c} \qquad (11)$$

where,

$$\omega_c = \frac{1}{\tau_c} = \frac{1}{CR} \qquad (12)$$

The input is shown connected to signal-earth because the switching process is governed by the parameters of the feed-

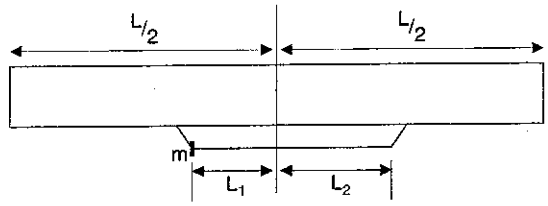

Fig. 11. Plan view of a see-saw, with weight m at an end-stop on a side rail.

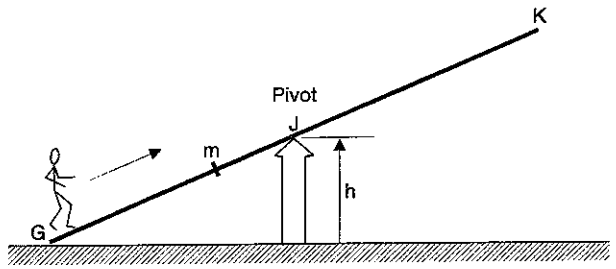

Fig. 12. Side view of see-saw, with person starting to walk from G to K.

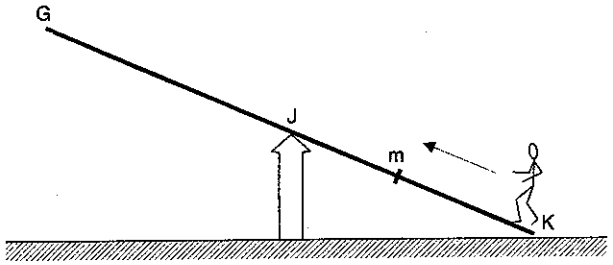

Fig. 13. The person starts to walk back from K to G.

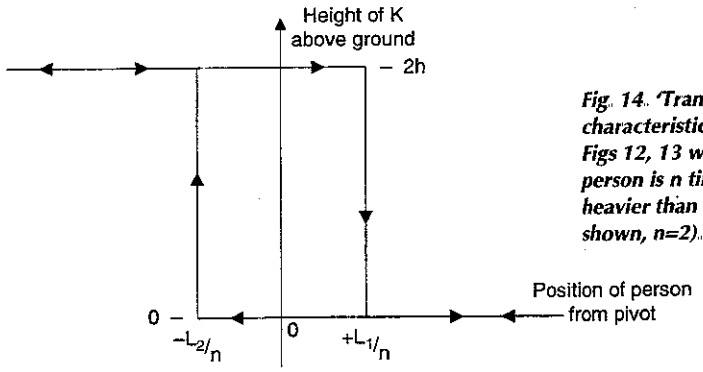

Fig. 14. 'Transfer characteristic' for Figs 12, 13 when person is n times heavier than m. (As shown, n=2).

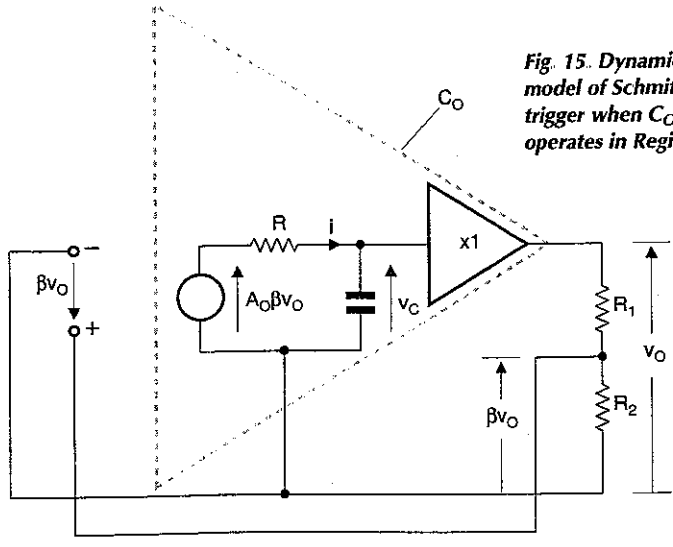

Fig. 15. Dynamic model of Schmitt trigger when C_O operates in Region 2.

back loop, not the input signal.

The charging current, i, for C is given by

$$i = C\frac{dv_C}{dt} = (A_O\beta - 1)\frac{v_O}{r} \quad (13)$$

or,

$$\frac{dv_O}{dt} = (A_O\beta - 1)\frac{v_O}{\tau_C} \quad (14)$$

Equation 14 follows from 13 by using eqn 12 and the fact that $v_O = v_C$.

A general solution of eqn 14 is of the form,

$$v_O \propto \exp(A_O\beta - 1)\frac{t}{\tau_C} \quad (15)$$

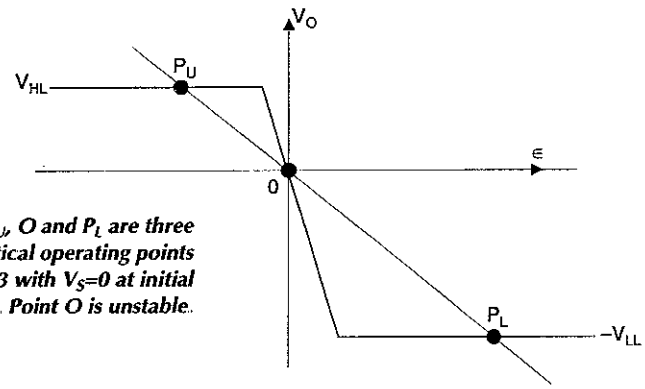

Fig. 16. P_U, O and P_L are three theoretical operating points for Fig. 3 with V_S=0 at initial switch-on. Point O is unstable.

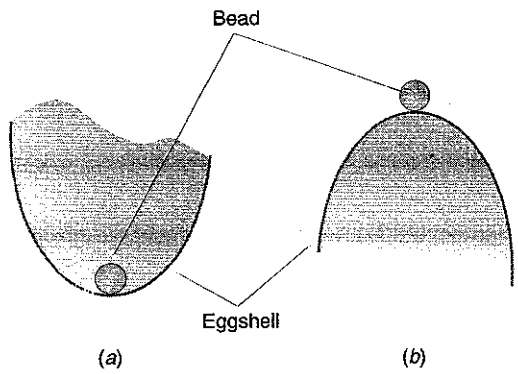

Fig. 17. (a) and (b) are mechanical analogues for stable and unstable equilibrium, respectively.

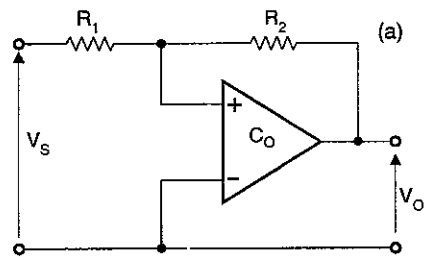

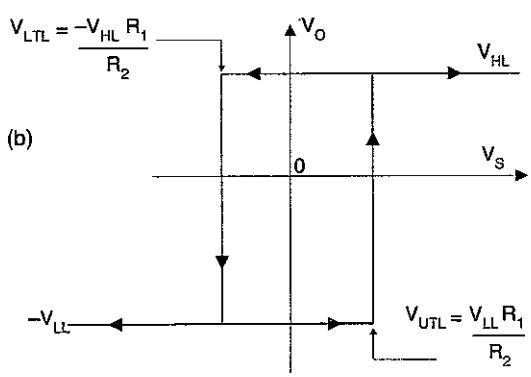

Fig. 18. A non-inverting Schmitt trigger, (a), its transfer characteristic, (b), and its preferred, unambiguous, symbol, (c).

Provided the loop-gain factor $A_O\beta$ exceeds unity, as is the case here, this equation describes an exponential growth once Region 2 is reached. In fact, eqn 15 is characteristic of the switch-over process not only in bistables but also monostables and astables

Switch-over time t_S is proportional to the time constant $\tau_C/(A_O\beta-1)$, but $\Delta V_H \propto \beta$ so t_S and ΔV_H are inversely related. It is *not* possible to have, simultaneously, zero hysteresis and regenerative switching – a fact overlooked by some authors

The condition $A_O\beta >> 1$ implies $A_O >> 1/\beta$. A graphical interpretation of this is that the fastest switching is obtained with the greatest angle between the slope of the operating line and the slope of the transfer characteristic in Region 2.

For the circuit of Fig. 3, there is a remaining problem to consider. What happens if V_S=0 when the circuit is initially switched on?

Direct-current conditions are satisfied at point O in **Fig. 16**. However, this is not stable. Referring to eqn 14, if $v_O > 0$ then $(dv_O/dt) > 0$ and operation moves to P_U: if, however, $v_O < 0$, then $(dv_O/dt) < 0$ and operation moves to P_L. So, following switch-on, $V_O = V_{HL}$ or $V_O = -V_{LL}$. It is impossible to say which it will be in advance. This is true at switch-on for any V_S lying between V_{LTL} and V_{UTL}.

In practice, eqn 15 is only approximately true because there is a non-linear relationship between V_O and ϵ in Region 2, which leads to daunting mathematics.

The differing conditions of stability at points P_1, P_3, in Fig. 5, are well-illustrated by the mechanical analogues in **Fig. 17**. In Fig. **17a**), corresponding to P_1, a small spherical bead rests inside the bottom of a half-eggshell. It is a stable position of equilibrium because the bead returns to its initial position following a small disturbance.

Figure **17b**) corresponds to operation at P_3. The bead cannot be stable on top of the inverted eggshell because, even if it was possible to balance it there initially, it would fall down the side after a small disturbance

Design considerations

The operation of a Schmitt trigger in the non-inverting mode, **Fig. 18a**), is similar to that described for the inverting mode. Its graphical analysis resembles that associated with Fig. 5.

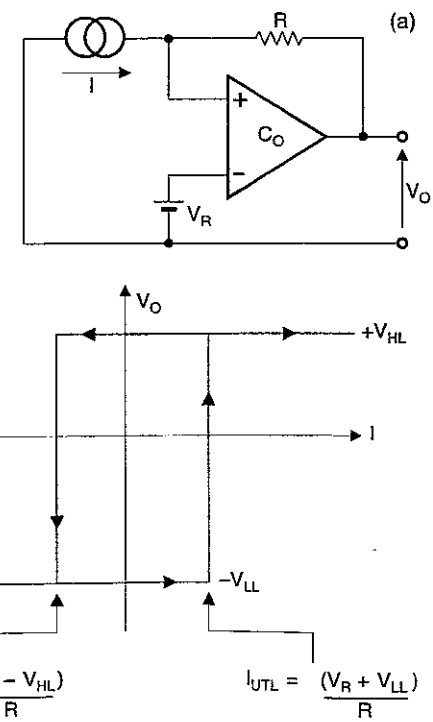

Fig. 19. (a) A current-comparing Schmitt trigger and (b) its transfer characteristic.

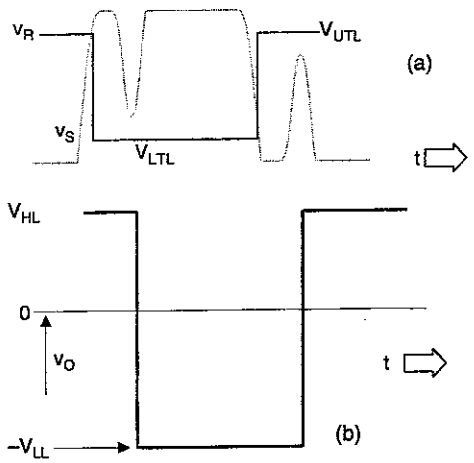

Fig. 20. Diagram (a) shows required location of V_{UTL} and V_{LTL} on comparator switched-reference level v_R to eliminate spikes p, q of Fig. 1b) while (b) shows the spike-free output waveform.

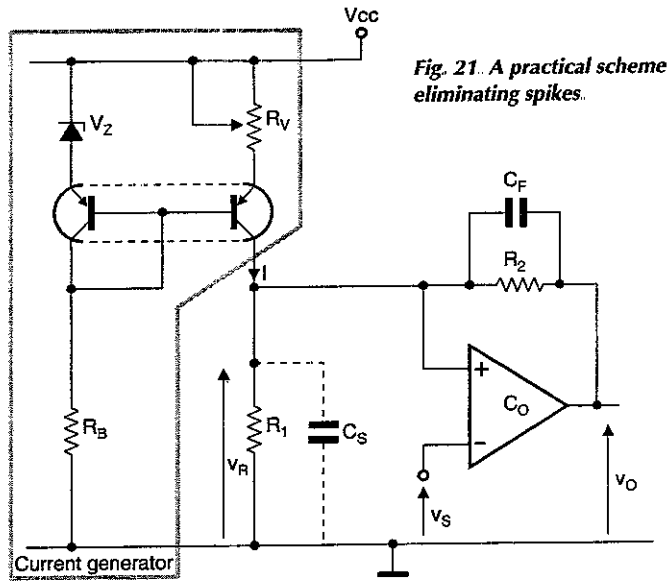

Fig. 21. A practical scheme for eliminating spikes.

For a given V_S, the operating line, still has a slope $-1/\beta$ but it passes through a point $\epsilon=-V_S(R_1+R_2)/R_2$ on the horizontal axis rather than $\epsilon=V_S$.

With increasing V_S, the line moves from right to left and *vice versa*. Consequently, $V_{UTL}=V_{LL}(R_1/R_2)$ and $V_{LTL}=-V_{HL}(R_1/R_2)$ and the hysteresis characteristic is shown in Fig **18b)**. An unambiguous block schematic representation[3] is shown in Fig. **18c)**. The hysteresis symbol in the box is reversed for inverting operation.

The non-inverting scheme does not provide the same degree of isolation from the driving source as the inverting configuration. This is because the output resistance, R_S, of the source must be included with R_1 for trip level calculations. When R_S is very large or poorly defined, a better procedure is to design for inverting operation and follow with an inverting buffer stage.

Applying a fixed reference potential to the inverting input of Fig. 18a) has the effect of shifting the hysteresis loop bodily along the horizontal axis as is evident with the current-comparing trigger shown in **Fig. 19**.

Returning now to the problem of logic spike elimination mentioned at the beginning of this article, the effect of p, q in Fig 1 can be avoided if the waveform is applied to an inverting trigger circuit with trip levels located as shown in **Fig. 20a)**: the output is then as shown in Fig. **20b)**.

It might be possible to achieve this using a standard monolithic Schmitt trigger such as the TTL 7413, which has V_{UTL} fixed at 1.9V and V_{LTL} at 0.9V. When a standard unit is not applicable a suitable scheme[4], a development of Fig. 3, is shown in **Fig. 21** in which v_S is the waveform of Fig. 1b).

Resistors R_1, R_2 are chosen so that,

$$V_{UTL}-V_{LTL}=\Delta V_H>(v_Q-v_P)$$

Current I is approximately V_Z/R_V. It is supplied by the circuit within the contour shown and provides a facility for shifting the hysteresis loop along the axis by a voltage $I(R_1//R_2)=IR_X$ without changing ΔV_H.

The design equations and design procedure are as follows.

$$V_{OH}>V_{UTL}>v_Q \tag{16}$$

or,

$$V_{OH}>(IR_X+\beta V_{HL})>v_Q \tag{17}$$

and,

$$v_P>V_{LTL}>V_{OL} \tag{18}$$

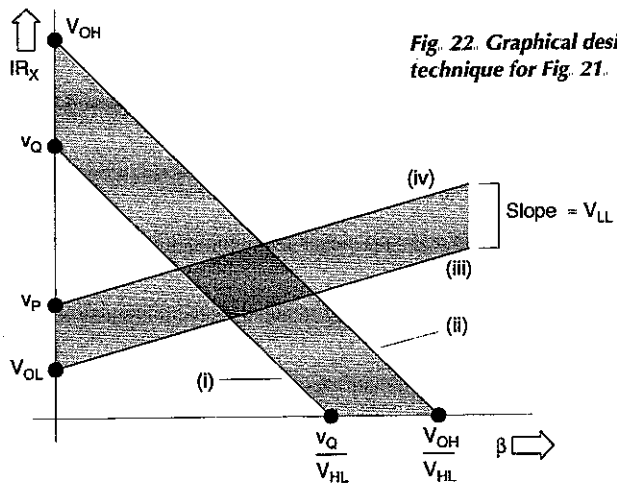

Fig. 22. Graphical design technique for Fig. 21.

i.e.,

$$v_P>(IR_X-(V_{LL})>V_{OL} \tag{19}$$

On a plot of IR_X versus β, **Fig. 22**, condition (17) is satisfied if the operating point lies between the parallel lines (i), (ii) and condition (19) is satisfied for operation between parallel lines (iii), (iv)

The cross-hatched area thus defines parameter choices for satisfactory operation. To allow for tolerances in R_1, R_2, I, etc , it is advisable to operate at a point in the centre of the permitted area. If this area encompasses the β axis it is possible to design for I=0.

This procedure only works precisely if C_O has a low output resistance at both of its output levels, as is the case with the long-established 710 comparator. The 311 requires an output pull-up resistor but, provided this is less than one tenth the resistance of R_2, the procedure given is still a useful starting point.

One further point; the speed-up capacitor C_F, in Fig. 21, is chosen to make the feedback network a compensated potentiometer so $C_FR_2=C_SR_1$, capacitance C_S being the total capacitance appearing across R_1.

Reversing the roles of the current generator and the feedback network in Fig 21 gives the circuit variation in **Fig. 23**. The design equations in this case are:

$$V_{UTL}=\beta V_{CC}+IR_X \tag{20}$$

$$V_{LTL}=\beta V_{CC} \tag{21}$$

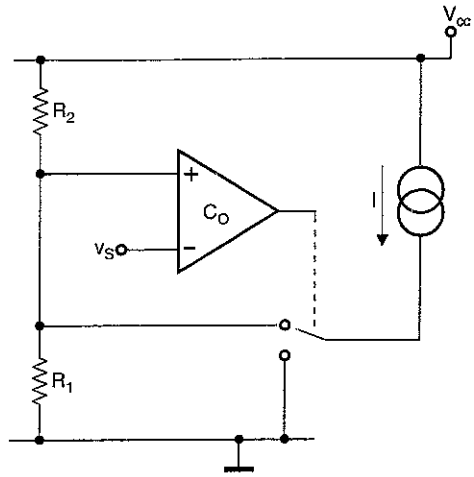

Fig. 23. A circuit variation of the technique of Fig. 21.

A graphical procedure, similar to that of Fig. 22, is applicable.

The design problems associated with Fig. 3 are eased and the resulting circuit is made more versatile if its two functions, trip-level definition and bistable-action, are performed separately as in the scheme of **Fig. 24**.

The common input signal for the comparators C_{O1}, C_{O2} is the waveform of Fig. 1b). The comparison potentials applied to them are, respectively, V_X, V_Y shown in Fig. 2a).

When $v_S<V_Y$ the bistable is set and remains set till $v_S>V_X$, when it is reset. This scheme allows free choice of V_{LTL}, V_{UTL} and provides both polarities of output. It is at the heart of the popular 555 timer IC.

When the device is used as an astable, the hysteresis voltage serves to define the voltage swing across a timing capacitor connected to the common input to the comparators. ■

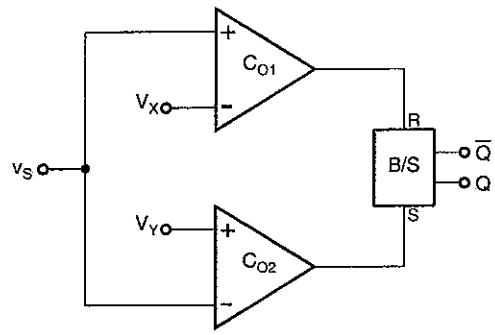

Fig. 24. Alternative Schmitt trigger configuration for spike elimination: V_X, V_Y are the voltage levels shown in Fig. 2a).

References

1 Schmitt O.H., 'A thermionic trigger', Journal of Scientific Instruments, 15, pp. 24-26 (1938).

2 Hart B.L., Introduction to Analogue Electronics' Arnold, Chapter 8 (1997).

3 IEE, 'Units and Symbols for Electrical and Electronic Engineering', IEE Guide (1997).

4 Hart B.L., 'A Schmitt trigger design technique for logic-noise-spike elimination' IJEEE, 21 pp 353-356, (1984).